Fatigue properties of solution strengthened ferritic ductile cast irons in heavy section castings

T. Borsato, P. Ferro, F. Berto, C. Carollo

Recently, standardized solution strengthened ferritic ductile cast irons (SSF-DI) have met the interest of the industrial world due to their improved mechanical properties and workability compared to standard ferritic-pearlitic ductile cast irons. However, the limited number of experimental data and the lack of production experience make the introduction of these new alloys to the market very difficult. For this reason, mechanical and fatigue properties of heavy section SSF-DI castings have been examined. Metallographic analyses have been performed using optical microscopy to identify the most important microstructural parameters. Fracture surfaces of fatigue specimens have been investigated using a Scanning Emission Microscope in order to identify crack initiation and propagation zones. Fatigue curves of SSF-DI have been finally compared with those obtained from traditional ductile cast iron specimens taken from the same casting geometry.

KEYWORDS: SOLUTION STRENGTHENED FERRITIC DUCTILE CAST IRONS, MICROSTRUCTURE, FATIGUE STRENGTH, DEFECTS, MECHANICAL PROPERTIES, HEAVY SECTION CASTING

INTRODUZIONE

In the last years, the production of heavy section cast iron components has had a significant increase due to the good mechanical properties and castability which allows to obtain very complex geometries in the as cast conditions. Traditional ferritic/pearlitic ductile cast irons have been studied since long; as known, a pearlitic matrix gives to the material high strength, while a ferritic matrix is characterized by high ductility. Recently, new generation ductile cast irons have met the interest of the industrial world. These types of materials are characterized by a fully ferritic matrix, solid solution strengthened through the addition of specific amount of silicon. The ferritic matrix gives high ductility, while the strengthening allows reaching good values of ultimate tensile strength and yielding strength in the as-cast condition, without the need of thermal treatments. Moreover, ferritic ductile cast irons strengthened by silicon addition have higher Rp0.2/Rm ratio and higher elongation at fracture than conventional ferritic, ferritic/pearlitic and pearlitic ductile cast irons at the same level of tensile strength. SSF DI exhibits also very small hardness variation due to their single-phase metal matrix, resulting in improved machinability and low tool wear. In literature (Larker et al. [1], De la Torre et al. [2], Stets et al. [3], Alhussein et al. [4] and Glavas et al [5]) it is reported that, increasing the silicon content from 2.4 wt% to 4.3 wt%, tensile strength, yield strength and hardness increase, while elongation at failure decreases. This behaviour is due to the decrease in plasticity and increase of embrittlement of ferrite strengthened by solid solution. Fatigue behaviour of SSF DI has been studied in some recent works ([2, 3] Okunnu [6], Bergström et al. [7], Alhussein et al. [8], Olsson [9] and Borsato et al.[10]). It was found that the fatigue resistance of solution strengthened ferritic grade is higher than that of traditional ferritic/pearlitic ductile cast irons at the same tensile strength.
In all the materials, microstructural defects, such as microshrinkage porosities or degenerated graphite particles, were found to be the causes for the fatigue crack initiation. Some authors [3, 6, 11], studied the effect of increased silicon content on the formation of microstructural defects. They concluded that increasing the amount of silicon, the ten-

T. Borsato, P. Ferro
University of Padova, Department of Engineering and Management, Stradella S. Nicola, 3 I-36100 Vicenza, Italy

F. Berto
NTNU, Department of Engineering Design and Materials, Richard Birkelands vei 2b, 7491, Trondheim – Norway

C. Carollo
VDP Fonderia SpA, via lago di Alleghe 39, 36015 Schio, Italy

dency for chunky graphite formation also increases in the thermal center of large castings, with detrimental effects on the mechanical properties. In particular, Källbom et al. [12] found that chunky graphite has negative effect on ultimate tensile strength and elongation at failure, but did not affect the yield strength and hardness of solution strengthened ferritic ductile cast irons.

While microstructural, mechanical and fatigue properties of traditional ductile cast irons in the presence of long solidification times have been quite well studied in the last years (Ferro et al. [13, 14], Mourujärvi et al. [15], Foglio et al. [16], Borsato et al. [17,18]), unfortunately, to the best of authors knowledge, only a work in literature [10] is focused on the mechanical and fatigue characterization of heavy section SSF ductile cast iron castings.

Considering the increased production of heavy section castings and the limited data available, the aim of this paper is to evaluate the effect of different amount of silicon and antimony on the microstructure, defects formation and mechanical behaviour of solution strengthened ferritic ductile cast irons, characterized by long solidification time. Moreover, the obtained results are compared with those obtained from traditional ductile cast irons under the same cooling conditions.

EXPERIMENTAL PROCEDURES

The materials under investigation were three different solution strengthened ferritic ductile cast irons, named D, G and H, which final chemical compositions are reported in Table 1. In particular, for casting D, the amount of silicon was 3.2 wt%, while for castings G and H the silicon content was higher and equal to 3.5 wt% and 3.55 wt%, respectively. As suggested in UNI EN 1563:2012 standard, with increasing the silicon content, the carbon content has been decreased correspondingly in order to maintain a near-eutectic composition. Carbon equivalent has been evaluated according to the well-known equation: C_{eq}=C%+0.33(Si%+P%). Moreover, for D and G castings, 15 ppm of Sb was added to the alloys in order to evaluate the effect of this element on counteracting the formation of Chunky graphite in the thermal center of heavy section castings. For casting H, Sb it was not used. The furan sand mould contained 4 blocks 300x250x300 mm3 in dimensions with feeders on top surfaces. Each block was sectioned in order to obtain specimens for mechanical and fatigue tests from the areas that take longer to solidify, characterized by solidification times of about 3 hours. Tensile tests have been carried out at room temperature according to UNI EN 1563:2012 standard both on separately cast samples (75 mm in thickness) and on specimens taken from the castings. Fatigue life tests were conducted at room temperature using a universal MTS machine (250 kN) applying uniaxial tension with frequency of 15 Hz and load ratio R=0. Fracture surfaces of broken specimens have been investigated using a Field Emission Gun – Environmental Scanning Electron Microscope (FEG-ESEM) (FEI, Quanta 250 FEG). The aim was to identify crack initiation sites and propagation zones. Metallographic analyses have been performed using an optical microscope interfaced with an image analysis software in order to identify the most important microstructural parameters. Results obtained for SSF DIs have been finally compared with those found in previous works by the same authors.

Tab. 1 - Final chemical composition of the castings

Casting	C	Si	S	P	Mn	Sb	Mg	Ceq
D	3.18	3.22	0.007	0.022	0.19	0.0015	0.043	4.26
G	3.14	3.50	0.007	0.026	0.19	0.0015	0.058	4.31
H	3.10	3.55	0.007	0.025	0.19	-	0.060	4.30

RESULTS AND DISCUSSIONS

Microstructure

To evaluate microstructural features, metallographic analyses have been carried out in a section of specimens taken from the inner of the castings. With the aim to identify matrix structure, samples have been etched with Nital 5%. Micrographs taken from castings D and G (Figure 1) showed homogeneous structure with spheroidal graphite nodules within a ferritic matrix, with limited traces of pearlitic areas, due to segregation of carbide forming elements.

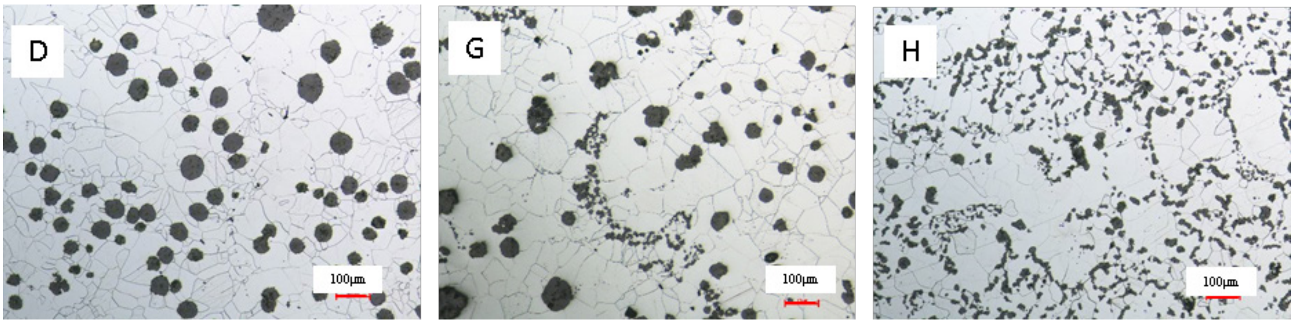

Fig. 1 - Micrographs of specimens from casting D, G and H

Some microstructural defects have been found, such as microshrinkage porosities and few amount of branched and interconnected degenerated graphite, classified as chunky graphite (CHG), slightly higher in the case of casting G. This seems to confirm that the increase of silicon content could promotes the formation of this type of graphite degenerated form. However, due to the limited amount of CHG in castings D and G, the treatment with Antimony is effective in preventing the formation of such a defect. As a matter of fact, in the centre of casting H, that was not treated with Sb, a great amount of Chunky graphite has been found (see Figure 1).

Static mechanical properties

In order to evaluate mechanical properties of the three different materials, tensile tests have been performed on specimens cut from separately cast samples according to UNI EN 1563:2012. The values obtained for tensile strength, yield strength and elongation at failure are shown in Table 2. It can be noted that the material is characterized by a very good compromise between strength and ductility. High ratio between yield and ultimate tensile stress and also a high value of elongation at failure have been found. It can also be observed that, as reported in the introduction, increasing the amount of silicon (from 3.2 to 3.55 wt%), ultimate tensile strength and yield stress increase, while elongation at failure decreases.

With the purpose to evaluate the influence of solidification times on mechanical properties, 10 tensile specimens for each casting have been taken from the zone with the longest solidification times. In Table 2, tensile test results from castings are also reported. It can be noted that, also in the case of long solidification times, considering casting D and G, the increased amount of silicon increases the strength and decreases the ductility. It is worth noting that standard deviation values are very limited, deducting that mechanical properties are very homogeneous in the whole castings. In the case of casting H, due to the presence of Chunky graphite, ultimate tensile strength and mostly elongation at failure showed a considerable reduction with respect to casting G, at similar silicon content.

Values obtained for SSF DI have been also compared with data coming from standard ferritic-pearlitic DIs. It has been found that, considering the properties inside the casting, SSF DIs show ultimate tensile strengths and yield stresses comparable with those found for the pearlitic grades, while maintaining high ductility (typical of traditional ferritic grade).

Tab. 2 - Tensile test results of specimens taken from separated cast samples and from the castings for solution strengthened ferritic, pearlitic and ferritic ductile cast irons

Casting	75 mm separated samples			Specimens from castings		
	σ_R [MPa]	σ_y [MPa]	ε_R %	σ_R [MPa]	σ_y [MPa]	ε_R%
D (SSF DI)	565	424	17.8	485.3 ± 1.8	381.2 ± 2.7	17.8 ± 1.0
G (SSF DI)	601	450	15.4	511.1 ± 3.0	412.3 ± 2.9	15.4 ± 1.7
H (SSF DI)	614	458	15.1	488.6 ± 7.9	430.4 ± 1.8	5.2 ± 1.1
Pearlitic	735	425	4.1	513.8 ± 10.1	368.6 ± 4.0	2.0 ± 0.2
Ferritic	400	262	23.4	383.1 ± 7.4	250.3 ± 4.2	19.9 ± 2.3

Fatigue tests and fractography

The results of fatigue tests have been statistically elaborated and the curves relative to survival probability of 10%, 50% and 90% were calculated using log-normal distribution. The run out specimens that have passed two million cycles, and specimens failed before $1 \cdot 10^4$ cycles were not included in the statistical analysis. In Figures 2-3-4, the fatigue curves of each casting are shown with the scatter band defined by the lines at survival probability of 10% and 90%.

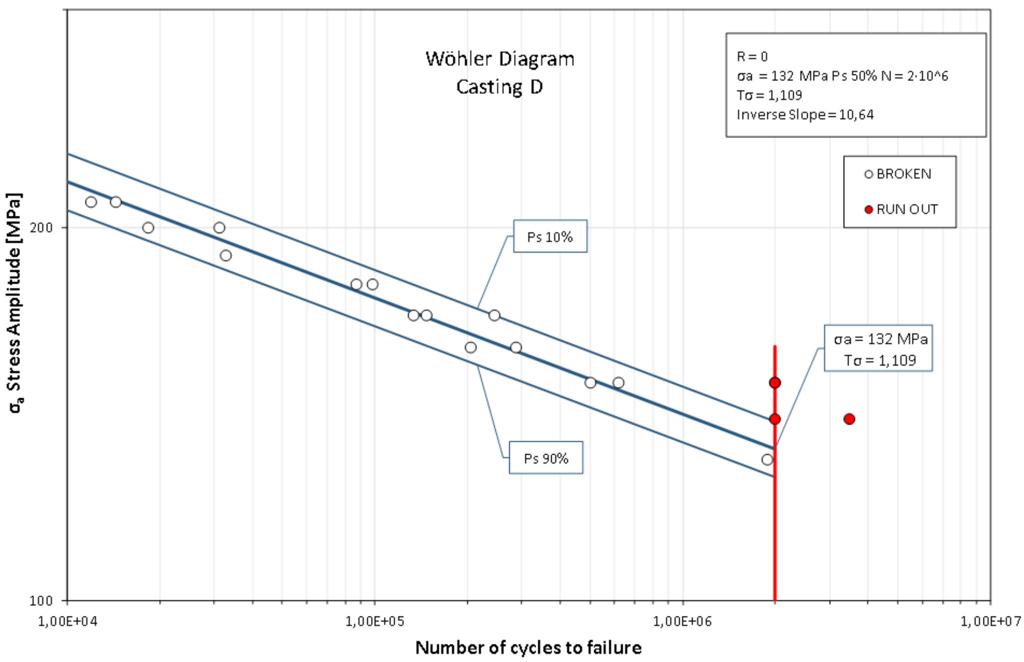

Fig. 2 - Fatigue life of specimens taken from casting D

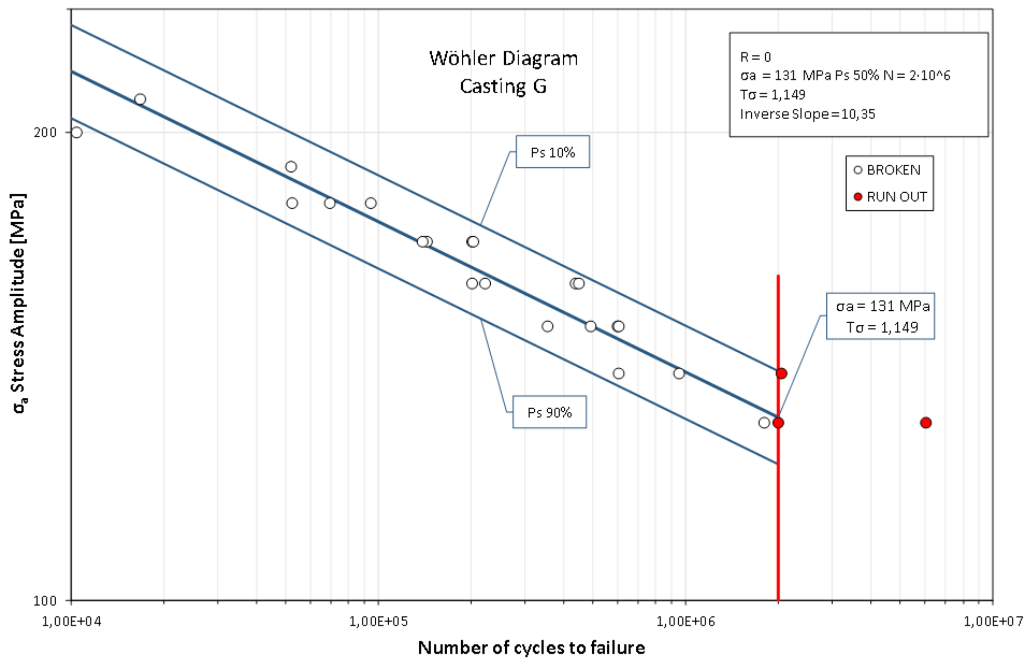

Fig. 3 - Fatigue life of specimens taken from casting G

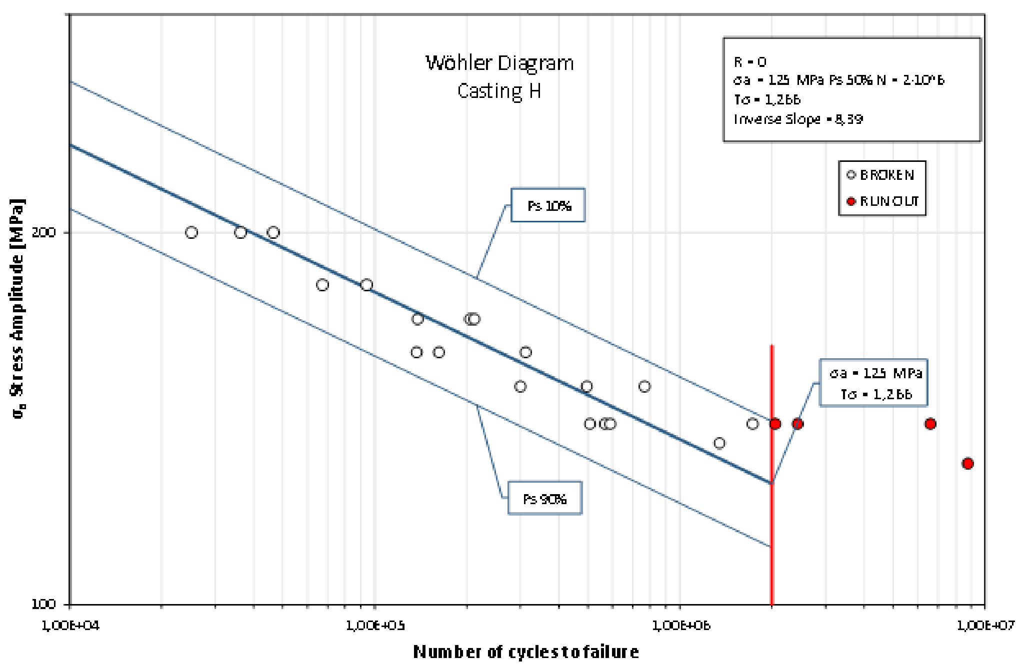

Fig. 4 - Fatigue life of specimens taken from casting H

The mean stress amplitudes relative to a survival probability of 50% at two million cycles, the scatter index and the slope, are also reported. It can be noted that, although the differences in the mechanical properties, the fatigue behaviour of D and G castings is similar, in terms of fatigue limit, slope of the curve and scatter index T_σ. It is important to highlight that, considering the higher tensile and yield strength of casting G, one would expect also a higher fatigue resistance. Finally, the fatigue limit of casting H, which contains high amount of chunky graphite, has been found to be slightly lower than the previous castings. Differences have been also observed in the slope of the fatigue curve. Fracture surfaces of broken specimens have been investigated using a Scanning Election Microscope in order to identify crack initiation (Figure 5a and b) and propagation zones (Figure 5c and d).

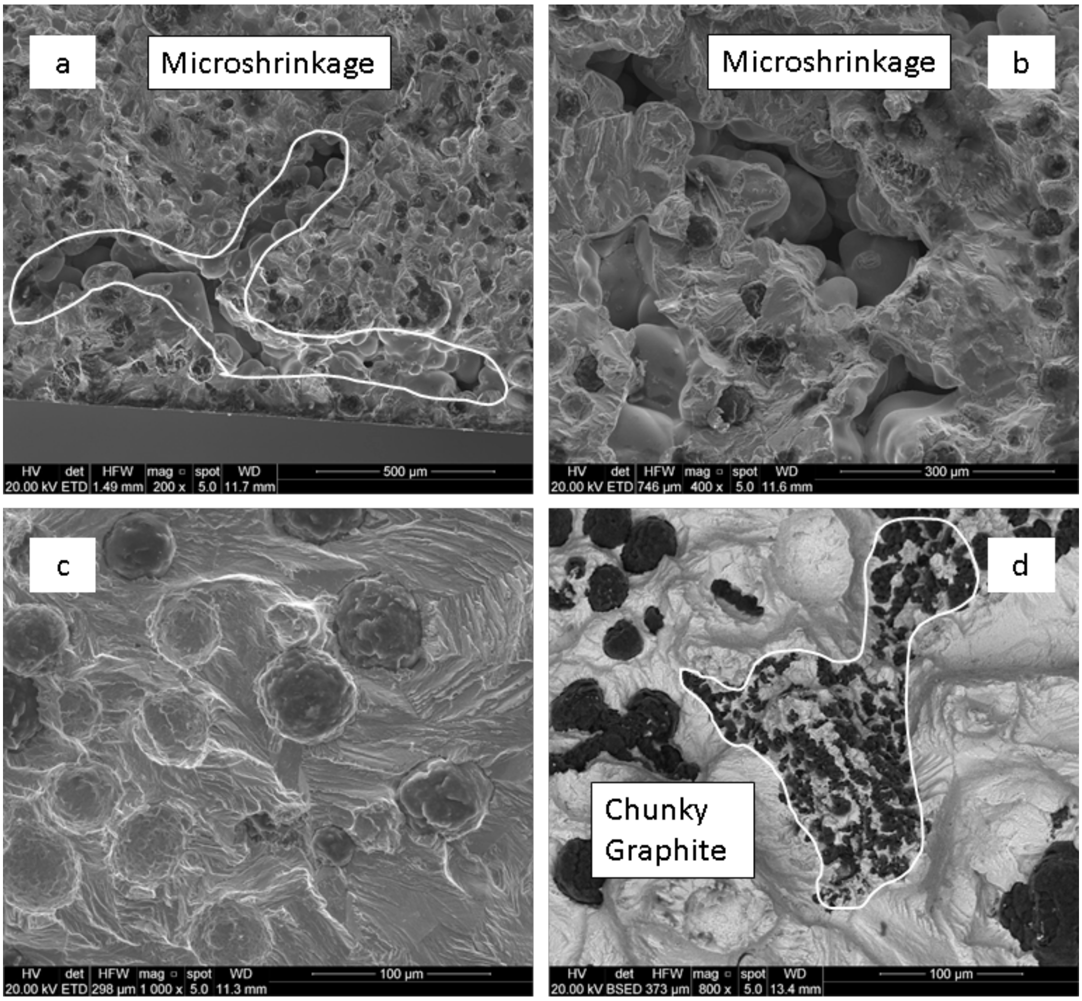

Fig. 5 - SEM micrographs of crack initiation, showing microshrinkage porosity (a,b), propagation zones in the presence of spheroidal graphite (c) and chunky graphite (d)

As reported in other works [10, 14-18], all the samples showed shrinkage porosities, even of large dimensions, near the surface which have been identified as cracks initiation points. It has been also observed that such cavities are similar in size between the castings. The main differences have been found in the crack propagation areas. While, in the case of casting D, the fatigue crack growth occurred along the graphite nodules/matrix interface, which slow the propagation, in the G and H specimens, the crack propagates easily through the areas with branched and interconnected degenerated graphite particles. This phenomenon is also shown in figure 6, where a cross sectional view of the fracture surface shows that fatigue crack passes around the graphite nodule while propagates through the chunky graphite (CHG).

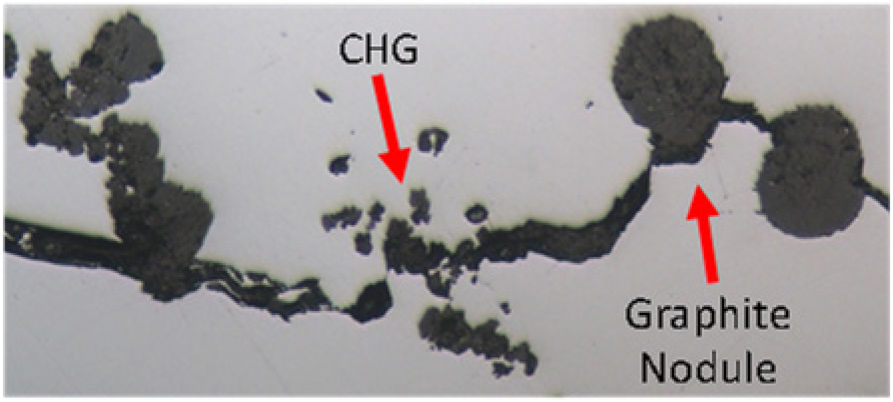

Fig. 6 - Cross sectional view of the fracture surface showing that fatigue crack passes around the graphite nodule while propagates through the chunky graphite (CHG)

In the authors' opinion, this mechanism could be the cause of a reduction of the fatigue limit. It is worth noting that, as reported in [14-16], the amount of Chunky graphite visible in the fracture surface of fatigue specimens is always higher than that observed in metallographic samples, taken in a cross section near the rupture, highlighting that CHG is a preferential easy path for the propagation of the fatigue crack with respect to nodular graphite containing areas.
Further work has been done to compare the fatigue results of solution strengthened ferritic ductile cast irons with those of traditional ferritic and pearlitic grades obtained from the same casting geometry. Data have been taken from previous works [13, 17]. The fatigue test results of pearlitic and SSF ductile cast irons have been considered all together in the statistical elaboration (Figure 7), due to their similar behaviour under cyclic loading conditions. It has been found a fatigue limit equal to 126 MPa and a scatter index $T\sigma = 1.23$. The ferritic grades, on the contrary, have been only superimposed to the Wöhler diagram, due to the lower fatigue resistance, in order to have a graphical comparison of the fatigue behaviour of the three different ductile cast irons.

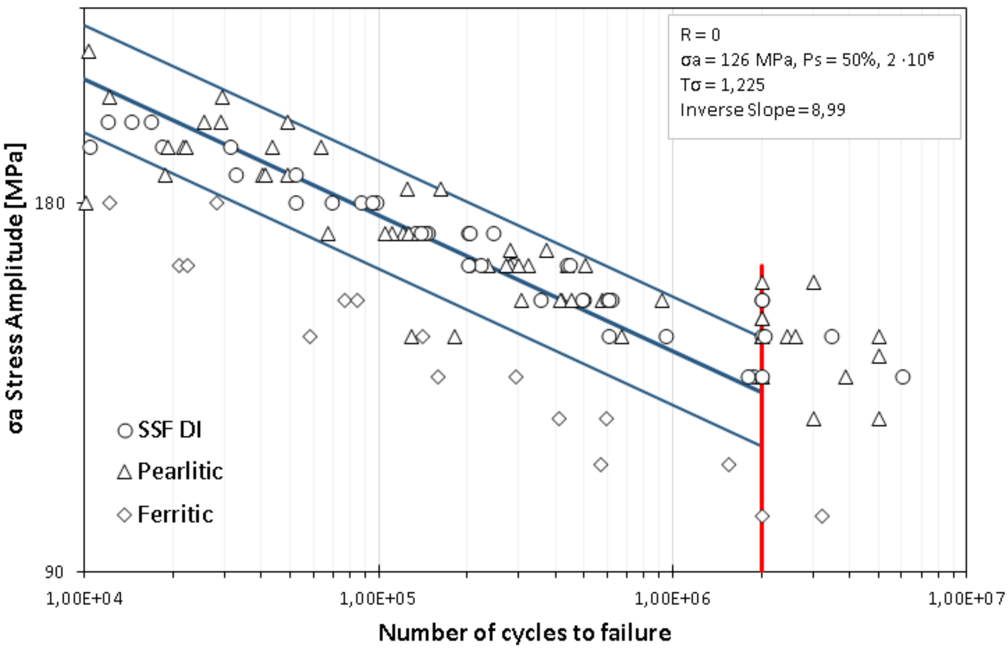

Fig. 7 - Fatigue life of specimens taken from pearlitic, ferritic and solution strengthened ferritic heavy section ductile cast iron castings

It can be noted that all the results are located within a narrow scatter band, highlighting the fact that, when considering long solidification times and slow cooling rates, although the difference in the structure, the SSF and the pearlitic DIs behave in a similar way, not only under static (Table 2), but also under dynamic loading conditions.

CONCLUSIONS

In this paper, the influence of different amount of silicon and antimony on static and fatigue properties of solution strengthened ferritic ductile cast irons characterized by a solidification time of about three hours has been investigated. It has been found that the increase of silicon content could promote the formation of degenerated Chunky graphite in the thermal centre of heavy section castings. However, it has been observed the treatment with antimony is effective in preventing the formation of such a defect. An increasing amount of silicon content from 3.2 to 3.55 wt% increases the ultimate tensile strength and yield stress, while decreases elongation at failure also in the presence of slow cooling rates. Due to the presence of Chunky graphite, ultimate tensile strength and ductility showed a great reduction. It has been also found that, considering long solidification times, SSF DIs have strength similar with that found for the pearlitic grades, while ductility comparable to the typical values of a traditional ferritic grades. Specimens taken from heavy section solution strengthened ferritic ductile cast iron castings behave in a similar way than the pearlitic grades under cycling loading conditions. All the samples showed shrinkage porosities, even of large dimensions and near the surface, which have been identified as cracks initiation points. In the presence of Chunky graphite, the crack propagates easily through the areas with branched and interconnected degenerated graphite particles, lowering the fatigue resistance.

ACKNOWLEDGMENTS

The authors would like to thank VDP Fonderia SpA for the material supply, financial and technical support to the project.

REFERENCE LIST

[1] Larker, R., China Foundry, Vol.6, No 4, 2009, pp. 343-351.

[2] De la Torre, U., Loizaga, A., Lacaze, J., and Sertucha, J., Mater. Sci. Technol. Vol. 30, No 12, 2014, pp. 1425-1431.

[3] Stets, W., Loblich, H., Gassner, G. and Schumacher, P., Int. J. Met. Vol. 8, 2014, pp. 35-40.

[4] Alhussein, A., Risbet, M., Bastien, A., Chobaut, J. P., Balloy, D.and Favergeon, J. Mater. Sci. Eng. A, Vol. 605, 2014, pp. 222-228.

[5] Glavas, Z., Strkalj, A.and Stojakovic, A., Metalurgija, Vol. 55, 2016, pp. 293-296.

[6] Okunnu, R., High Strength Solution Strengthened Ferritic Ductile Cast Iron. Master Thesis, Aalto University, 2015.

[7] Bergström, J., Burman, C., Svensson, J., Jansson, A., Ivansson, C., Zhou, J., and Valizadeh, S., Steel Res. Int. Vol. 87, 2016, pp. 614-621.

[8] Alhussein, A., Risbet, M., and Favergeon, J., Matec Web Conf. Vol. 12, 2014, pp. 1-4.

[9] Olsson, A., Fatigue strength of truck components in cast iron, Chalmers University of Technology, Goteborg, Sweden, 2011.

[10] Borsato, T. Ferro, P., Berto, F. and Carollo, C., Adv. Eng. Mat. Vol. 18, Issue 12, 2016, pp. 2070-2075.

[11] Nakae, H., Fukami, M., Kitazawa, T., and Zou, Y., China Foundry, Vol. 8, 2010, pp. 96-100.

[12] Källbom, R., Hamberg, K., Wessén, M. and Björkegren. L. E., Mater. Sci. Eng. A, Vol. 414, 2005, pp. 346-351.

[13] Ferro, P., Fabrizi, A., Cervo, R. and Carollo, C., J. Mat. Pro. Tech., Vol. 213, 2013, pp. 1601-1608.

[14] Ferro, P., Lazzarin, P., Berto, F., Mater. Sci. Eng. A, Vol. 554, 2012, pp. 122-128.

[15] Mourujärvi, A., Widell, K., Saukkonen, T. and Hänninen, H., Fatigue Fract Eng M, Vol. 32, 2009, pp. 379-390.

[16] Foglio, E., Lusuardi, D., Pola, A, La Vecchia, G.M. and Gelfi, M., Mater. Design, Vol. 111, 2016, pp. 353-361.

[17] Borsato, T., Berto, F., Ferro, P. and Carollo, C., Procedia Structural Integrity, Vol. 2, 2016, pp. 3150-3157.

[18] Borsato, T., Ferro, P, Berto, F. and Carollo, C., Int. J. Fatigue, Vol, Vol. 102, 2017, pp. 221-227.